Analysis of multijet events produced at high energy hadron colliders

S. Geer
Fermi National Accelerator Laboratory, P.O. Box 500, Batavia, Illinois 60510

T. Asakawa
University of Tsukuba, Tsukuba, Ibaraki 305, Japan
(Received 12 October 1995)

We define and discuss a set of $(4N-4)$ parameters that can be used to analyze events in which N jets have been produced in high-energy hadron-hadron collisions. These multijet variables are the multijet mass and $(4N-5)$ independent dimensionless parameters. To illustrate the use of the variables QCD predictions are presented for events with up to five jets produced at the Fermilab Tevatron proton-antiproton collider. These QCD predictions are compared with the predictions of a model in which multijet events uniformly populate the N-body phase space. [S0556-2821(96)01609-8]

PACS number(s): 12.38.Qk, 13.85.Hd, 13.87.Ce

I. INTRODUCTION

Large samples of events containing two or more jets have recently been recorded at the Fermilab Tevatron proton-antiproton collider. Many of the observed events contain three, four, or even five or more jets [1]. A comprehensive analysis of these multijet events would provide an interesting test of leading-order (LO) perturbative quantum chromodynamics (QCD) $2\rightarrow N$ calculations. In the last few years complete LO QCD matrix elements have become available for $N=3$ [2], $N=4$ [3], and $N=5$ [4]. Partial calculations exist for $N>5$ [5]. The $2\rightarrow N$ calculations are complicated, and have required the development of new techniques [6]. Unfortunately the computing resources needed to evaluate the matrix elements increase rapidly with N. A considerable effort has therefore been devoted to finding approximations to the exact LO matrix elements that permit faster calculations [7]. A comprehensive analysis of multijet events at high-energy hadron colliders can provide a test of any approximations that may be used in present or future $2\rightarrow N$ calculations. Finally, in addition to providing a test of the QCD calculations, a detailed understanding of the properties of multijet events produced in high-energy hadron-hadron collisions is important because multijet production is expected to be prolific in future high luminosity running at the Fermilab proton-antiproton collider and at the Large Hadron Collider (LHC) at CERN. A comprehensive understanding of QCD multijet production is therefore required to facilitate the search for more exotic processes producing multijet events. For example, a detailed understanding of the properties of six-jet events at the Fermilab collider is likely to be important in the near future for the study of $t\bar{t}$ production and decay in the all hadronic channel.

In the past, elegant analyses of two-jet and three-jet production have been published by the UA1 [8,9] and UA2 [10,11] collaborations at the CERN Super Proton Synchrotron ($S\bar{p}pS$) Collider and by the Collider Detector at Fermilab (CDF) [12,13] and D0 [14] Collaborations at the Fermilab Tevatron collider. There have also been analyses of events with more than three jets [14–16]. However, the analyses of events with four or more jets have not used a simple set of independent variables that (i) span the multijet parameter space, (ii) make it simple to interpret the observed event distributions within the framework of perturbative QCD, and (iii) make it easy to compare the characteristics of events having N jets with the characteristics of events having for example $(N+1)$ jets. In this paper we discuss a set of multijet parameters that satisfy these criteria. It is hoped that a complete set of multijet variables that enable a comparison between the properties of N-jet and $(N+1)$-jet events will facilitate (a) a more comprehensive analysis of multijet events, and (b) a more comprehensive test of any approximations used in the QCD calculations.

In choosing a set of multijet variables that span the multijet parameter space it should be noted that we can completely define a system of N massive bodies in the N-body restframe by specifying the $4N$ components of four-momentum. The N-body system would then be overspecified since momentum conservation provides us with three constraints. Furthermore, we can rotate the N-body system about the incoming beam direction without loosing any interesting information. Therefore, to describe the system we need only specify $(4N-4)$ parameters. We will take these parameters to be the N-body mass and $(4N-5)$ additional variables. We therefore introduce and discuss a set $(4N-5)$ dimensionless variables which, in the addition of the multijet mass, span the multijet parameter space. Our $(4N-5)$ multijet variables will provide a simple framework within which the properties of multijet events can be compared with QCD predictions.

In previous analyses observed multijet distributions have been compared with predictions from LO QCD matrix element calculations and/or predictions from parton shower Monte Carlo programs. Therefore, to illustrate the use of our multijet variables and test the agreement between the matrix element and parton shower Monte Carlo calculations, in this paper we compare the predictions from exact LO QCD matrix element calculations with the corresponding predictions from a QCD parton shower Monte Carlo program, and from a model in which the events are uniformly distributed over the available N-body phase space. The QCD and phase-space calculations are described in Sec. II. In Sec. III the analysis

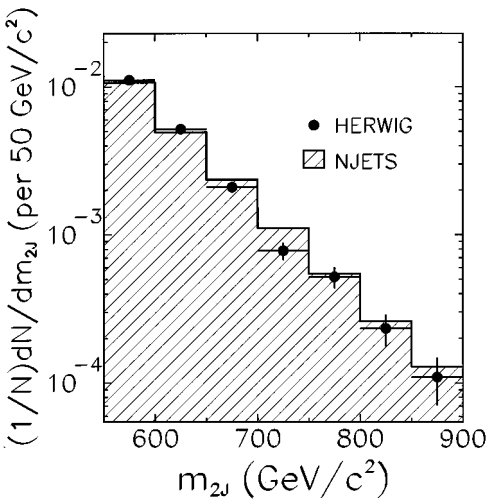

FIG. 1. Predicted two-jet mass distributions for two-jet events produced at the Fermilab proton-antiproton collider. HERWIG (points) compared with NJETS (histogram) after applying the requirements of $m_{2J}>550$ GeV/c^2 and $|\cos\theta^*|<0.6$.

of two-jet events is briefly discussed. The standard three-jet variables are reviewed and extended in Sec. IV. Four-jet and five-jet variables are introduced and discussed in Secs. V and VI. In Sec. VII the generalization of the multijet parameters to describe topologies with more than five jets is discussed. Finally, a summary is given in Sec. VIII.

II. QCD AND PHASE-SPACE PREDICTIONS

To illustrate the use of our multijet variables we will present and discuss various predictions for the distribution of multijet events in the multijet parameter space. In particular we will consider two-jet, three-jet, four-jet, and five-jet events produced at the Fermilab proton-antiproton collider operating at a center of mass energy of 1.8 TeV, and compare predictions obtained from (a) the HERWIG [17] QCD parton shower Monte Carlo program, (b) the NJETS [4] LO QCD $2\rightarrow N$ matrix element Monte Carlo program, and (c) a model in which events are distributed uniformly over the available N-body phase space.

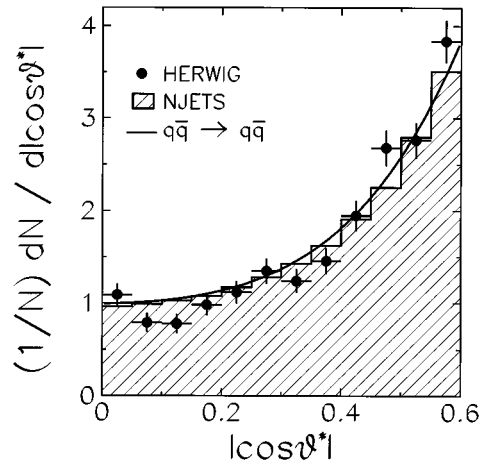

FIG. 2. Predicted $|\cos\theta^*|$ distributions for two-jet events produced at the Fermilab proton-antiproton collider that satisfy the requirements $m_{2J}>550$ GeV/c^2 and $|\cos\theta^*|<0.6$. The HERWIG prediction (points) is compared with the NJETS prediction (histogram), and the LO QCD prediction for $(q\bar{q}\rightarrow q\bar{q})$ scattering (curve).

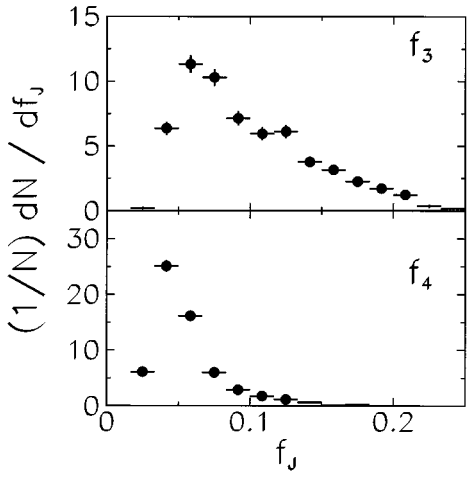

FIG. 3. The HERWIG Monte Carlo predictions for the distributions of leading and next-to-leading single-jet-mass fractions for jets in two-jet events produced at the Fermilab proton-antiproton collider that satisfy the requirements $m_{2J}>550$ GeV/c^2 and $|\cos\theta^*|<0.6$.

A. Jet definitions and selection criteria

The QCD and phase-space model predictions depend upon the algorithm used to define jets and selection criteria used to define the data sample. To illustrate the use of our multijet variables we will take as an example jet definitions and event selection criteria recently used by the CDF Collaboration to define a multijet data sample recorded at the Fermilab proton-antiproton collider [1]. Our predictions will therefore be for an existing data sample. Following the CDF prescription, jets are defined such that they satisfy the following: (i) jet transverse energy $E_T>20$ GeV, where

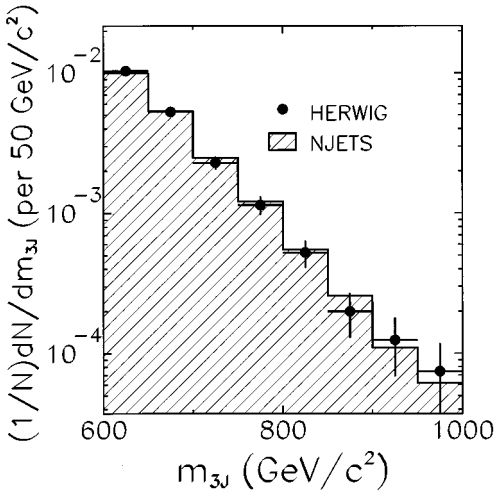

FIG. 4. Predicted three-jet mass distributions for events produced at the Fermilab proton-antiproton collider that satisfy the requirements $m_{3J}>600$ GeV/c^2, $X_3<0.9$, and $|\cos\theta_3|<0.6$. HERWIG predictions (points) are compared with NJETS predictions (histogram).

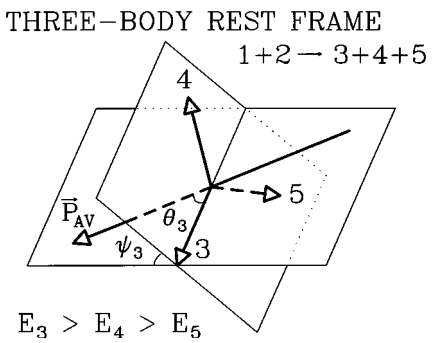

FIG. 5. Schematic definition of angles used to describe the three-jet system in the three-jet restframe.

$E_T \equiv E \sin\theta$, E is the jet energy, and θ is the angle between the jet and the beam direction in the laboratory frame, (ii) $|\eta|<3$, where the jet pseudorapidity $\eta \equiv -\ln\tan(\theta/2)$, and (iii) jet-jet separation $\Delta R>0.9$, where $\Delta R \equiv (\Delta\eta^2 + \Delta\phi^2)^{1/2}$, and $\Delta\eta$ and $\Delta\phi$ are the differences in pseudorapidity and azimuthal angle between the two jets.

With these jet definitions, the multijet event sample is defined by selecting events that satisfy the following: (a) total transverse energy $\Sigma E_T>420$ GeV, where the sum is over all jets with $E_T>20$ GeV, (b) multijet mass $m_{NJ}>m_{\min}$, and (c) the cosine of the leading-jet scattering angle $\cos\theta<(\cos\theta)_{\max}$ where the leading jet is defined as the highest energy jet in the multijet restframe.

Note that for two-jet events the ΣE_T requirements selects events with jet $E_T>210$ GeV. At fixed two-jet mass this results in an effective maximum allowed value of $\cos\theta$. The values of $m_{\min}$ and $(\cos\theta)_{\max}$ are chosen to restrict the parameter space to the region in which the ΣE_T requirement is efficient.

B. The HERWIG parton shower Monte Carlo calculation

HERWIG [17] is a QCD parton shower Monte Carlo program that includes both initial- and final-state gluon radiation. HERWIG predictions can be thought of as LO QCD $2\rightarrow2$ predictions with gluon radiation and QCD jet evolution in which soft-gluon interference is implemented via angular ordering. The HERWIG Monte Carlo program also includes color coherence of the initial- and final-state hard partons, backward evolution of initial-state partons including interference, hadronization of jets via nonperturbative gluon splitting, and an underlying event. We have used version 5.6 of the HERWIG Monte Carlo program, and defined jets by using a cone algorithm with a cone radius $\Delta R=0.7$. With this choice of cone radius we are effectively requiring that the minimum separation between jets $\Delta R_{\min}=0.9$, which is well matched to the explicit requirement $\Delta R>0.9$ described earlier. After using a cone algorithm to define jets we use a simple detector simulation that modifies the jet energies with a Gaussian resolution function with $\sigma_E=0.1E$. This is similar to the jet energy resolution function reported by the CDF

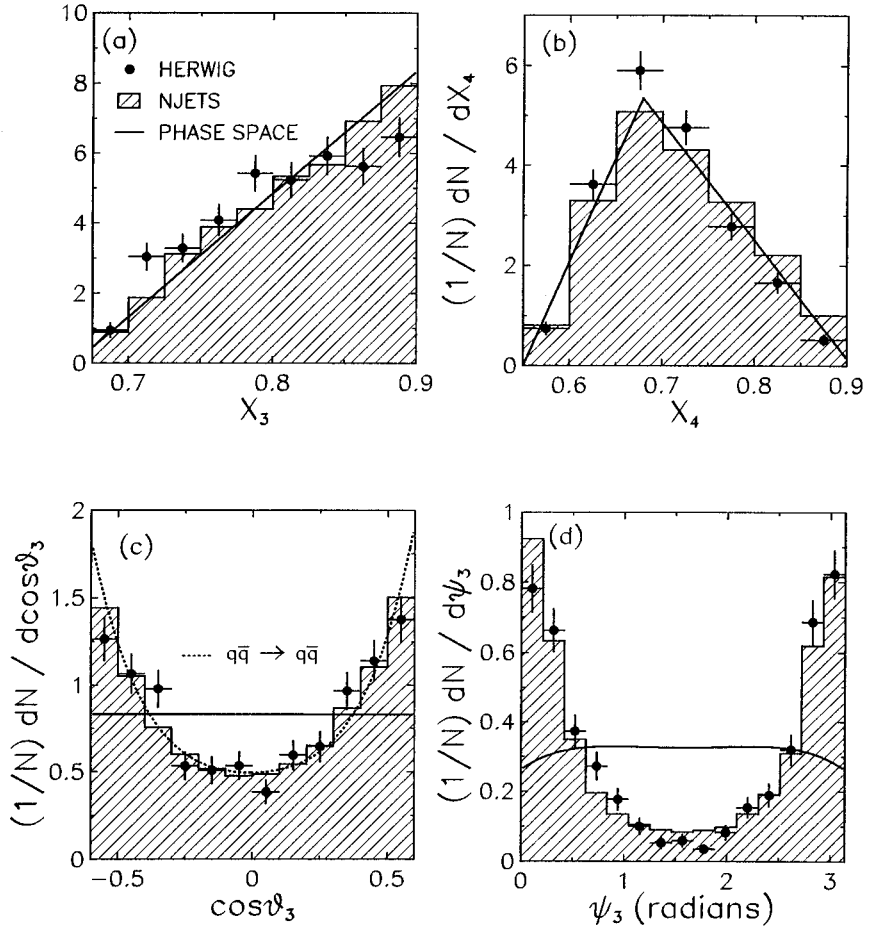

FIG. 6. Predicted distributions of the three-jet variables defined in the text for three-jet events produced at the Fermilab proton-antiproton collider that satisfy the requirements $m_{3J}>600$ GeV/c^2, $X_3<0.9$, and $|\cos\theta_3|<0.6$. HERWIG predictions (points) are compared with NJETS predictions (histograms) and the phase-space model predictions (solid curves) for (a) X_3, (b) X_4, (c) $\cos\theta_3$, and (d) ψ_3. The broken curve in the $\cos\theta_3$ figure is the LO QCD prediction for $q\bar{q}\rightarrow q\bar{q}$ scattering.

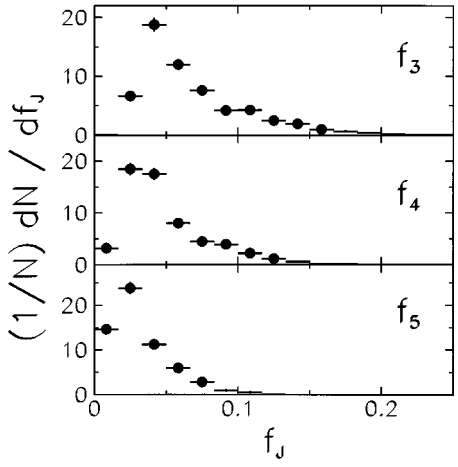

FIG. 7. HERWIG Monte Carlo predictions for the single-jet mass-fraction distribution for jets in three-jet events produced at the Fermilab proton-antiproton collider that satisfy the requirements $m_{3J}>600$ GeV/c^2, $X_3<0.9$, and $|\cos\theta_3|<0.6$.

Collaboration [1]. In our HERWIG calculations we have used the CTEQ1M [18] structure functions and the scale $Q^2=stu/2(s^2+u^2+t^2)$. HERWIG generates $2\rightarrow2$ processes above a specified $p_T^{\rm hard}$ where $p_T^{\rm hard}$ is the p_T of the outgoing partons from the hard scatter before any radiation has occurred. We have set the minimum $p_T^{\rm hard}$ to 60 GeV/c. Finally, the HERWIG Monte Carlo distributions discussed in this paper are inclusive. Hence, for a given jet multiplicity N, the generated events contribute to the distributions if they have at least N jets that pass the jet requirements. If there are more than N jets in a generated event, the multijet system is defined using the N highest E_T jets.

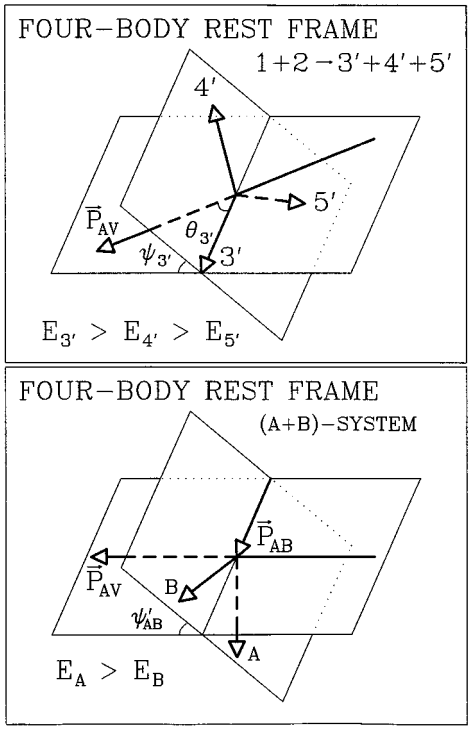

FIG. 8. Schematic definition of angles used to describe the four-jet system in the four-jet restframe.

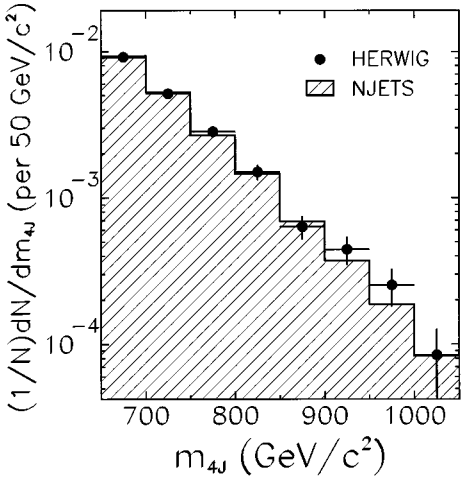

FIG. 9. Predicted four-jet mass distributions for events produced at the Fermilab proton-antiproton collider that satisfy the requirements $m_{4J}>650$ GeV/c^2, $X_{3'}<0.9$, and $|\cos\theta_{3'}|<0.8$. HERWIG predictions (points) are compared with NJETS predictions (histogram).

C. The NJETS QCD matrix element calculation

The NJETS Monte Carlo program [4] provides parton-level predictions based on the LO QCD $2\rightarrow N$ matrix elements. We have used the Kwiecinski-Martin-Roberts-Stirling set D0 (KMRSD0) structure function parametrization [19] with the renormalization scale chosen to be the average p_T of the outgoing partons. NJETS does not use a parton fragmentation model. Jet definitions and selection cuts are therefore applied to the final-state partons. To enable a direct comparison between NJETS and HERWIG predictions we have smeared the final-state parton energies in our NJETS calculations with the jet energy resolution function described above.

D. Phase-space model

We have generated samples of Monte Carlo events for which the multijet systems uniformly populate the N-body phase space. These phase-space Monte Carlo events were generated with single-jet masses distributed according to the single-jet mass distribution predicted by the HERWIG Monte Carlo program. In addition, the multijet mass distributions were generated according to the corresponding distributions obtained from the HERWIG Monte Carlo calculation. Comparisons between the resulting phase-space model distributions and the corresponding HERWIG and NJETS Monte Carlo distributions help us to understand which multijet parameters are most sensitive to the behavior of QCD multijet matrix elements.

III. TWO-JET VARIABLES

We begin by briefly reviewing the variables that are often used in two-jet analyses [8,10,12]. Consider a system of two massless jets. The massless jet approximation is appropriate because at high center-of-mass energies single-jet masses are much smaller than two-jet masses (m_{2J}). To describe a system of two massless jets in the two-jet restframe we need only two variables. In previous two-jet analyses these variables have often been chosen to be m_{2J} and $\cos\theta^*$, where

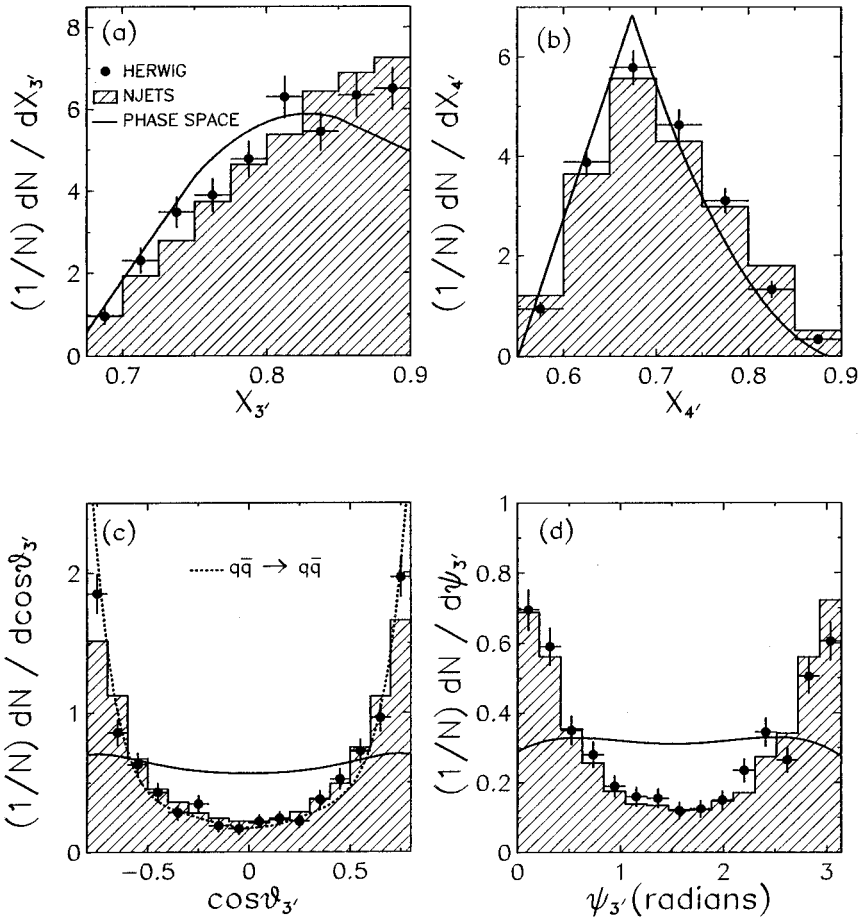

FIG. 10. Predicted distributions of three-body variables described in the text for four-jet events produced at the Fermilab proton-antiproton collider that satisfy the requirements $m_{4J}>650$ GeV/c^2, $X_{3'}<0.9$, and $|\cos\theta_{3'}|<0.8$. The HERWIG predictions (points) are compared with NJETS predictions (histograms), and with the phase-space model predictions (solid curves) for (a) $X_{3'}$, (b) $X_{4'}$, (c) $\cos\theta_{3'}$, and (d) ψ_3'. The broken curve in the $\cos\theta_{3'}$ figure is the LO QCD prediction for $q\bar{q}\rightarrow q\bar{q}$ scattering.

θ^* is the scattering angle between the incoming beam particles and the outgoing jets in the two-jet restframe. In defining $\cos\theta^*$ it must be remembered that in practice a two-jet system will always be produced together with a spectator system, and the incoming beam particles will not be collinear in the two-body rest-frame. Hence, following the convention of Collins and Soper [20] θ^* is taken to be the angle between the outgoing jets and the average beam direction. Consider the process $1+2\rightarrow 3+4$. The center-of-mass scattering angle is defined

$$\cos\theta^* \equiv \frac{\vec{P}_{\rm av}\cdot\vec{P}_3}{|\vec{P}_{\rm av}||\vec{P}_3|}, \tag{1}$$

where

$$\vec{P}_{\rm av}=\vec{P}_1-\vec{P}_2, \tag{2}$$

and we define particle 1 as the incoming interacting parton with the highest energy in the laboratory frame.

NJETS and HERWIG QCD Monte Carlo predictions for the m_{2J} and $\cos\theta^*$ distributions are shown in Figs. 1 and 2, respectively, for two-jet events produced at the Fermilab proton-antiproton collider satisfying the requirements $m_{2J}>550$ GeV/c^2 and $|\cos\theta^*|<0.6$. Note that in the HERWIG Monte Carlo calculation the jets acquire mass in the fragmentation process, whereas in the NJETS calculation jets are identified with massless partons. Hence the agreement

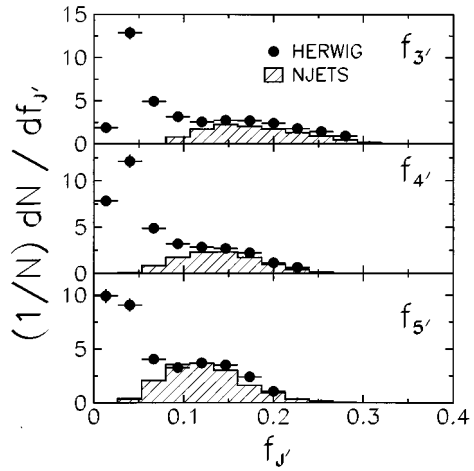

FIG. 11. The predicted distributions of single-jet mass fractions for jets in four-jet events produced at the Fermilab proton-antiproton collider that satisfy the requirements $m_{4J}>650$ GeV/c^2, $X_{3'}<0.9$, and $|\cos\theta_{3'}|<0.8$. HERWIG predictions (points) are compared with NJETS predictions (histograms).

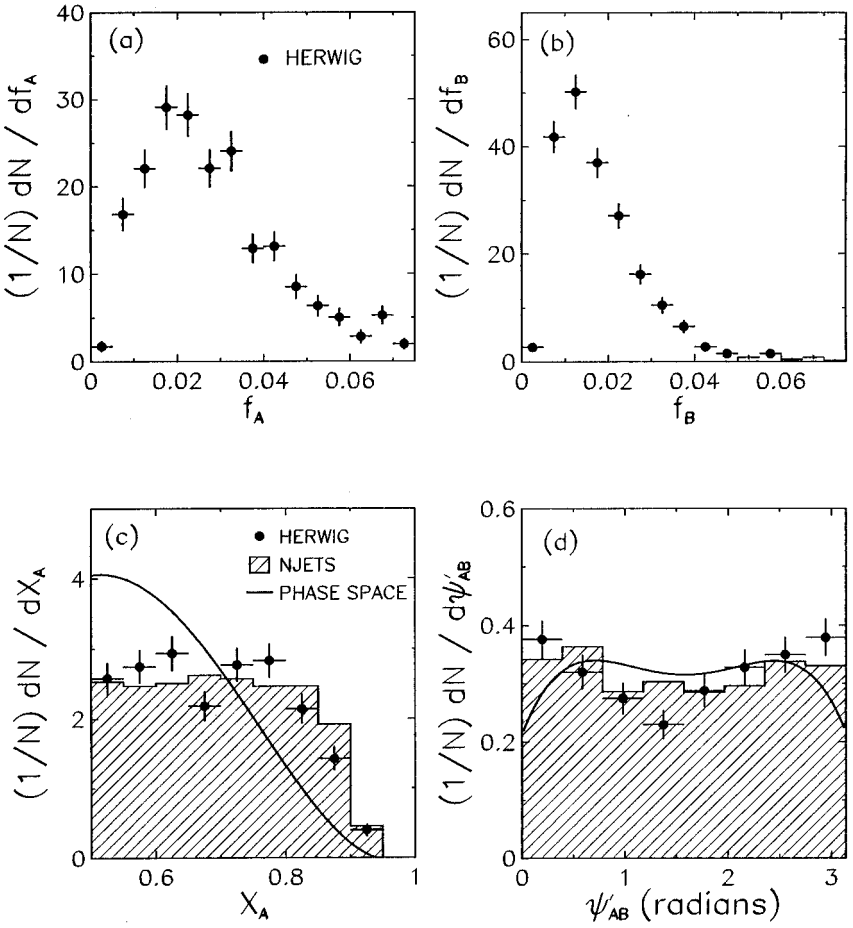

FIG. 12. The predicted distributions of the four-jet variables describing the (AB) system for four-jet events produced at the Fermilab proton-antiproton collider that satisfy the requirements $m_{4J}>650$ GeV/c^2, $X_{3'}<0.9$, and $|\cos\theta_{3'}|<0.8$. The HERWIG predictions (points) are compared with NJETS predictions (histograms), and the phase-space predictions (curves) for (a) f_A, (b) f_B, (c) X_A, and (d) ψ'_{AB}.

between the HERWIG and NJETS predictions shows amongst other things that the kinematic distributions are not sensitive to fragmentation effects. The predicted $\cos\theta^*$ distributions are similar to the angular distribution expected at LO for $q\bar{q}\to q\bar{q}$ scattering [21], which is not very different from the well-known Rutherford scattering form

$$\frac{d\sigma}{d\cos\theta^*}\simeq(1-\cos\theta^*)^{-2}. \tag{3}$$

Hence, the $\cos\theta^*$ variable has some nice features. First, the LO QCD prediction for the $\cos\theta^*$ distribution is well known and is similar, although not identical, to the Rutherford scattering distribution. Second, the phase-space density is independent of $\cos\theta^*$. Therefore the measured $\cos\theta^*$ distribution depends upon the underlying $2\to2$ matrix element in a very direct way.

To prepare for the analysis of system with many jets in the final state it is useful to extend the two-jet variables to describe two-jet systems with massive final-state jets. To do this we must specify two additional parameters. Obvious choices are the final-state single-jet masses m_3 and m_4. We prefer to use dimensionless variables, and therefore choose the single-jet mass fractions f_3 and f_4, defined by

$$f_j\equiv\frac{m_j}{m_{NJ}}, \tag{4}$$

where for two-jet events the mass of the multijet system $m_{NJ}=m_{2J}$. We order the jets in the two-body rest frame such that $E_3>E_4$, and hence $f_3>f_4$. The HERWIG predictions for the f_3 and f_4 distributions are shown in Fig. 3. Note that as expected f_3 and f_4 tend to be small, typically of order 0.05–0.1.

We conclude by noting that we have defined four variables that specify a two-jet system in the two-body rest-frame: m_{2J}, $\cos\theta^*$, f_3, and f_4.

IV. THREE-JET VARIABLES

In the standard three-jet analysis used by the UA1 Collaboration [9], and later by the CDF [13] and D0 [14] Collaborations, five variables are chosen that specify the system of three massless particles in the three-body restframe. The first of these variables is the three-jet mass (m_{3J}). The NJETS and HERWIG predictions for the m_{3J} distribution are shown in Fig. 4 to be in good agreement with each other. The predicted m_{3J} distributions have also recently been shown to be in good agreement with the observed CDF m_{3J} distribution [1]. To complete the description of the three-jet system four additional dimensionless variables are defined that, together with m_{3J}, span the three-body parameter space. In defining the three-jet parameters it is traditional to label the outgoing jets 3, 4, and 5, and order the jets such that $E_3>E_4>E_5$, where E_j is the energy of jet j in the three-jet restframe. The traditional three-jet variables employed are X_3, X_4, $\cos\theta_3$,

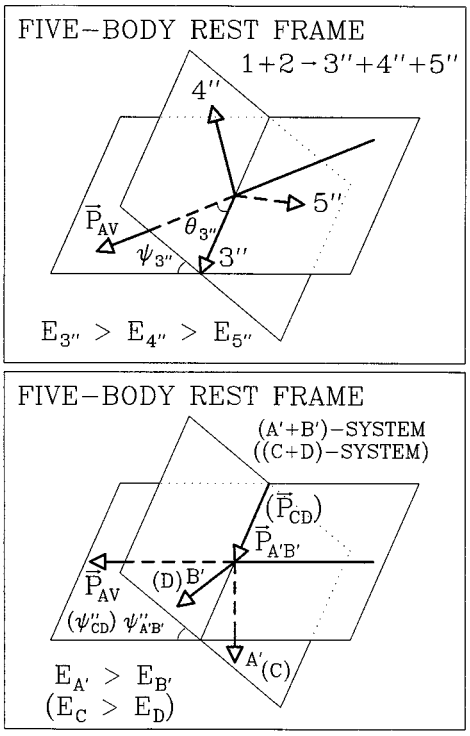

FIG. 13. Schematic definitions of angles used to describe the five-jet system in the five-jet restframe.

and ψ_3, which are defined as follows.

(i) X_j, the jet energy fractions, normalized:

$$X_j \equiv \frac{2E_j}{E_3+E_4+E_5} = \frac{2E_j}{m_{3J}}. \tag{5}$$

(ii) $\cos\theta_3$, defined in the three-jet rest-frame as the cosine of the leading-jet scattering angle (see Fig. 5):

$$\cos\theta_3 \equiv \frac{\vec{P}_{\rm av}\cdot\vec{P}_3}{|\vec{P}_{\rm av}||\vec{P}_3|}. \tag{6}$$

(iii) ψ_3, defined in the three-jet restframe as in the angle between the three-jet plane and the plane containing jet 3 (the leading jet) and the average beam direction (see Fig. 5):

$$\cos\psi_3 \equiv \frac{(\vec{P}_3\times\vec{P}_{\rm av})\cdot(\vec{P}_4\times\vec{P}_5)}{|\vec{P}_3\times\vec{P}_{\rm av}||\vec{P}_4\times\vec{P}_5|}. \tag{7}$$

Predictions for the X_3, X_4, $\cos\theta_3$, and ψ_3 distributions are shown in Fig. 6 for three-jet events produced at the Fermilab proton-antiproton collider that satisfy the requirements $m_{3J}>600$ GeV/c^2, $|\cos\theta_3|<0.6$, and $X_3<0.9$. These selection criteria are used to restrict the parameter space to the region for which the ΣE_T requirement is efficient and to ensure that the jets in the three-jet sample are well measured. The first and second three-jet parameters (X_3 and X_4) are Dalitz variables, normalized so that $X_3+X_4+X_5=2$. Momentum conservation restricts the ranges of the Dalitz variables (for massless jets $2/3\leqslant X_3\leqslant 1$ and $1/2\leqslant X_4\leqslant 1$). The phase-space density is uniform over the kinematically allowed region of the (X_3,X_4) plane, and hence the phase-space model predictions for the X_3 and X_4 distributions can be easily understood. Note that the QCD predictions for the X_3 and X_4 distributions are similar to those of the phase space model. We might have expected the QCD calculations to predict an enhanced event rate as $X_3\rightarrow 1$ and the three-jet system therefore approaches a two-jet configuration. However, in practice the algorithm used to define jets and the experimental requirements used to select well-measured three-jet events restrict the measured three-jet topologies to those that populate regions of the three-body phase space where the matrix element varies only slowly over the (X_3,X_4) plane. The third and fourth three-jet parameters ($\cos\theta_3$ and ψ_3) are angular variables. The phase-space density is uniform in $\cos\theta_3$ space, ψ_3 space, and is also uniform in the $(\cos\theta_3,\psi_3)$ plane. Indeed, the phase-space model does predict a uniform $\cos\theta_3$ distribution. The phase-space model prediction for the ψ_3 distribution is not quite uniform, there being a slight depletion of events as $\psi_3\rightarrow 0$ or π. This depletion is primarily a consequence of the minimum E_T requirement used to define jets. We would expect the QCD predictions for the two angular distributions to be very different from the phase-space model predictions. In particular we might expect that the leading-jet angular distribution would be similar, although not identical, to the LO $q\bar{q}\rightarrow q\bar{q}$ scattering form. Indeed, this is seen to be the case for both the NJETS and HERWIG QCD predictions [Fig. 6(c)]. We might also expect the initial-state radiation pole in the QCD matrix element to result in an enhanced rate of three-jet events for topologies in which the angle between the beam direction and the three-jet plane is small. Hence, we would expect the ψ_3 distribution to be peaked towards 0 and π. This is also evident in the HERWIG and NJETS predictions.

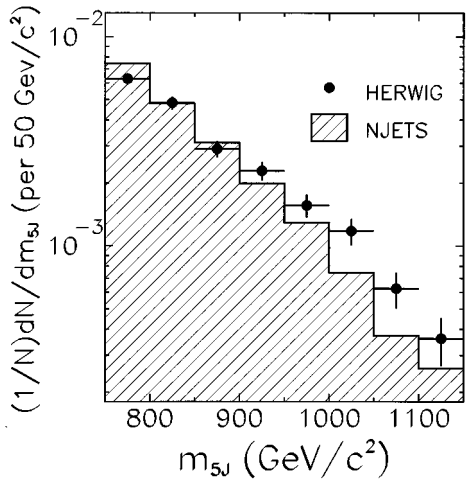

FIG. 14. Predicted five-jet mass distributions for five-jet events produced at the Fermilab proton-antiproton collider. HERWIG predictions (points) compared with NJETS predictions (histogram).

To prepare for the analysis of events with more than three jets we now wish to extend the three-jet variables to describe a system of three massive particles in the three-body restframe. To do this we must specify an additional three parameters, which we take to be the single-jet mass fractions f_3, f_4, and f_5. HERWIG predictions for f_3, f_4, and f_5 are shown in Fig. 7. Note that the f_j tend to be small, typically less than or of order 0.1.

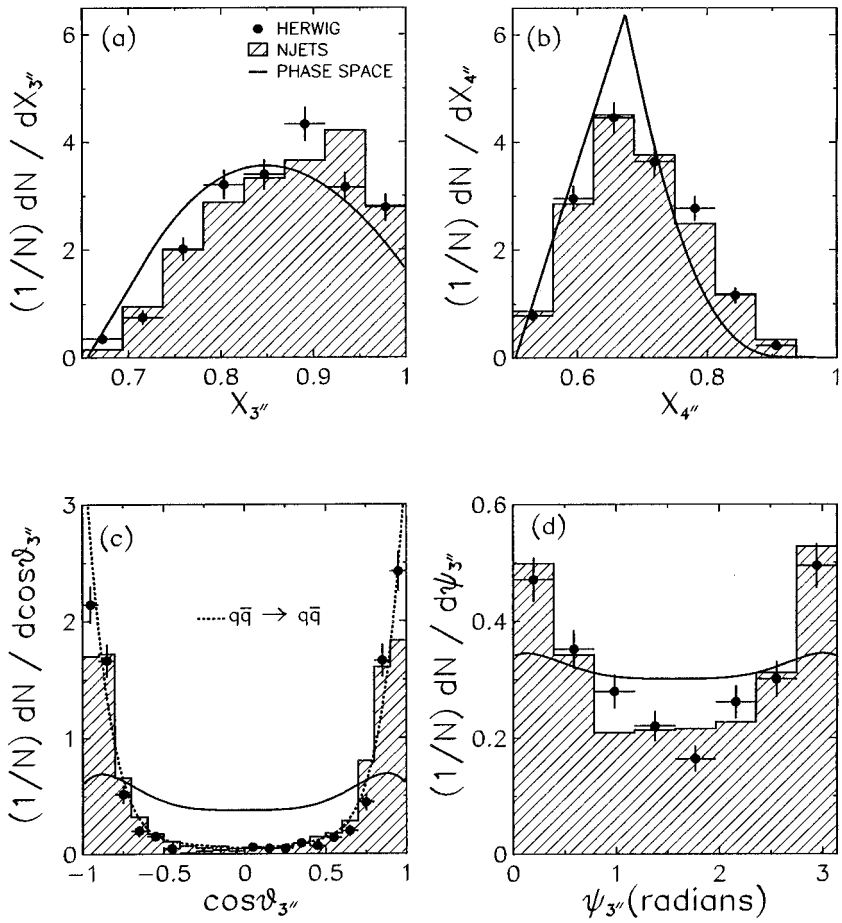

FIG. 15. Predicted distributions of three-body variables for five-jet events produced at the Fermilab proton-antiproton collider that satisfy the requirement $m_{5J}>750$ GeV/c^2. HERWIG predictions (points) are compared with NJETS predictions (histograms) and the phase-space predictions (solid curves) for (a) $X_{3''}$, (b) $X_{4''}$, (c) $\cos\theta_{3''}$, and (d) $\psi_{3''}$. The broken curve in the $\cos\theta_{3''}$ figure is the LO QCD prediction for $q\bar{q}\rightarrow q\bar{q}$ scattering.

We conclude by noting that we have defined eight variables that specify a three-jet system in the three-body restframe: m_{3J}, X_3, X_4, $\cos\theta_3$, ψ_3, f_3, f_4, and f_5.

V. FOUR-JET VARIABLES

To completely describe a system of four jets in the four-body restframe we must specify 12 independent parameters. We will choose the four-jet mass (m_{4J}) and 11 dimensionless variables that span the four-body parameter space. We have chosen a set of four-jet variables that, for four-jet configurations that approach a three-body topology, reduce to the three-jet variables discussed in the previous section. This will make it possible to compare the characteristics of four-jet events with the corresponding characteristics of three-jet events.

The four-jet variables are shown schematically in Fig. 8. We begin by reducing the four-jet system to a three-body system by combining the two jets with the lowest two-jet mass. We will label the two jets we combine A and B with $E_A>E_B$, where E_A and E_B are the jet energies in the four-jet restframe. After A and B have been combined, the resulting three bodies are labeled $3'$, $4'$, and $5'$, and are ordered in the three-body restframe so that $E_{3'}>E_{4'}>E_{5'}$. Note that we use a nomenclature in which primed labels denote objects which are defined after two jets have been combined. The three-body system can be completely specified using a generalization of the three-jet variables: $X_{3'}$, $X_{4'}$, $\cos\theta_{3'}$, $\psi_{3'}$, $f_{3'}$, $f_{4'}$, and $f_{5'}$. Explicitly, for a multijet system with mass m_{NJ} that has been reduced to three bodies (i,j,k), we define the following.

(i) X_i, the fraction of the three-body energy taken by object i, normalized:

$$X_i\equiv\frac{2E_i}{E_i+E_j+E_k}=\frac{2E_i}{m_{NJ}}. \tag{8}$$

(ii) $\cos\theta_i$, the cosine of the scattering angle for object i:

$$\cos\theta_i\equiv\frac{\hat{P}_{\rm av}\cdot\hat{P}_i}{|\vec{P}_{\rm av}||\vec{P}_i|}. \tag{9}$$

(iii) ψ_i, the angle between the three-body plane and the plane containing object i and the average beam direction:

$$\cos\psi_i\equiv\frac{(\vec{P}_i\times\vec{P}_{\rm av})\cdot(\vec{P}_j\times\vec{P}_k)}{|\vec{P}_i\times\vec{P}_{\rm av}||\vec{P}_j\times\vec{P}_k|}. \tag{10}$$

(v) f_i, the mass of object i divided by the three-body mass:

$$f_i\equiv\frac{m_i}{m_{NJ}}. \tag{11}$$

The NJETS and HERWIG predictions for the m_{4J} distribution are shown in Fig. 9 for four-jet events produced at the Fermilab proton-antiproton collider satisfying the requirements $m_{4J}>650$ GeV/c^2, $|\cos\theta_{3'}|<0.8$, and $X_{3'}<0.9$. The

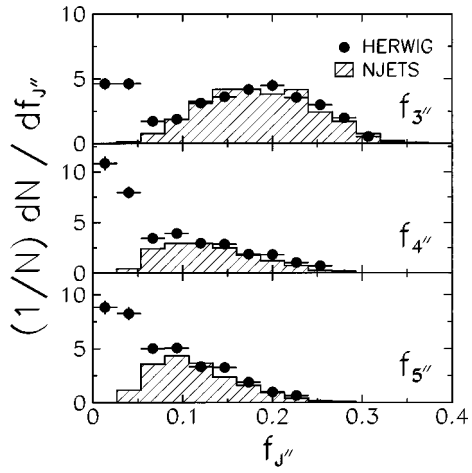

FIG. 16. Predicted distributions of the mass fractions described in the text for five-jet events produced at the Fermilab proton-antiproton collider that satisfy the requirement $m_{5J}>750$ GeV/c^2. HERWIG predictions (points) compared with NJETS predictions (histograms).

QCD predictions for the $X_{3'}$, $X_{4'}$, $\cos\theta$, and $\psi_{3'}$ distributions are compared with the phase-space model predictions in Fig. 10. There is reasonable agreement between the HERWIG and NJETS predictions for all of these distributions. The QCD predictions for the $X_{3'}$ and $X_{4'}$ distributions are not very different from the predictions of the phase-space model. In contrast, the NJETS and HERWIG $\cos\theta_{3'}$ and $\psi_{3'}$ distributions are very different from the more uniform phase-space model predictions. It is interesting to compare these distributions with the equivalent distributions for three-jet events (Fig. 6). The QCD and phase-space model predictions for the four-jet distributions are similar but not identical to the corresponding distributions for three-jet events. Note that (1) in comparing the phase-space model predictions for the X_3 and $X_{3'}$ distributions we see that the predicted $X_{3'}$ distribution is depleted at large $X_{3'}$, and (2) in comparing the phase-space model predictions for the X_4 and $X_{4'}$ distributions we see that the predicted $X_{4'}$ distribution is distorted at large $X_{4'}$. These differences can be qualitatively understood by noting that if $4'$ or $5'$ is the (AB) system and hence massive then $X_{3'}<1$ even if $4'$ and $5'$ are collinear. It should also be noted that the phase-space model $\cos\theta_{3'}$ distribution is slightly depleted at small $|\cos\theta_{3'}|$ and the $\psi_{3'}$ distribution is slightly depleted for values of $\psi_{3'}$ close to 0 and π. These features are consequences of the minimum jet-jet separation requirement $\Delta R>0.9$, and the minimum jet transverse energy requirement $E_T>20$ GeV.

The HERWIG predictions for the normalized masses are shown in Fig. 11. They exhibit peaks close to $f_i=0.05$ which reflect the finite single-jet masses resulting from the HERWIG fragmentation model, and long tails at larger values of f_i which reflect the contributions from the combined (AB) systems. Note that although single jets are massless in the NJETS calculation, the NJETS program does predict the contribution to the f_i distributions from the combined (AB) systems, and indeed the NJETS and HERWIG predictions are in good agreement at large f_i.

To complete our description of the four-jet system we must now specify four additional parameters that describe the two-jet (AB) system. To describe the (AB) system we choose (a) the single-jet mass fractions f_A and f_B, (b) X_A, defined in the four-jet restframe as the fraction of the energy of the (AB) system taken by the leading jet

$$X_A \equiv \frac{E_A}{E_A+E_B}, \tag{12}$$

and (c) ψ'_{AB}, defined in the four-jet restframe as the angle between (i) the plane containing the (AB) system and the average beam direction, and (ii) the plane containing A and B (see Fig. 8). The prime reminds us that in order to define ψ'_{AB} we have combined two jets to obtain the (AB) system. Note that

$$\cos\psi'_{AB} \equiv \frac{(\vec{P}_A\times\vec{P}_B)\cdot(\vec{P}_{AB}\times\vec{P}_{\rm av})}{|\vec{P}_A\times\vec{P}_B||\vec{P}_{AB}\times\vec{P}_{\rm av}|}. \tag{13}$$

The predicted f_A and f_B distributions are shown in Figs. 12(a) and 12(b), respectively. The typical values of f_A and f_B predicted by the HERWIG fragmentation model are less than or of order 0.05. The predicted X_A distributions are shown in Fig. 12(c). The NJETS and HERWIG QCD calculations yield harder X_A distributions than the corresponding distribution predicted by the phase-space model, reflecting the presence of the soft gluon radiation pole in the QCD matrix element. To gain some insight into the shape of the phase-space model prediction for the X_A distribution consider a system of four massless particles labeled randomly i, j, k, and l. If we define $X_i \equiv E_i/(E_i+E_j)$, then the phase-space prediction for the distribution of events as a function of X_i is given by

$$\frac{dN}{dX_i} \sim \frac{3}{X_i^2} - \frac{1}{X_i^3} - 2. \tag{14}$$

This function is already quite similar to the phase-space model prediction shown in Fig. 12(c), which is obtained by requiring that the (AB) system is the lowest mass pair, and taking account of finite single-jet masses and experimental selection requirements. Finally, the predicted ψ'_{AB} distributions are shown in Fig. 12(d). The NJETS and HERWIG predictions for the ψ'_{AB} distribution are in agreement with one another. The slight decrease in the population of events predicted by the phase-space model as ψ'_{AB} approaches 0 or π is a consequence of the minimum jet E_T requirement.

We conclude by noting that we have defined 12 variables that specify a four-jet system in the four-body restframe: m_{4J}, $X_{3'}$, $X_{4'}$, $\cos\theta_{3'}$, $\psi_{3'}$, $f_{3'}$, $f_{4'}$, $f_{5'}$, f_A, f_B, X_A, and ψ'_{AB}.

VI. FIVE-JET VARIABLES

To completely describe a system of five jets in the five-body restframe we must specify 16 independent parameters. We will choose the five-jet mass (m_{5J}) and 15 dimensionless variables that span the five-body parameter space. We have chosen a set of five-jet variables that, for five-body configurations that approach a four-body topology, reduce to the four-jet variables discussed in the previous section. Further-

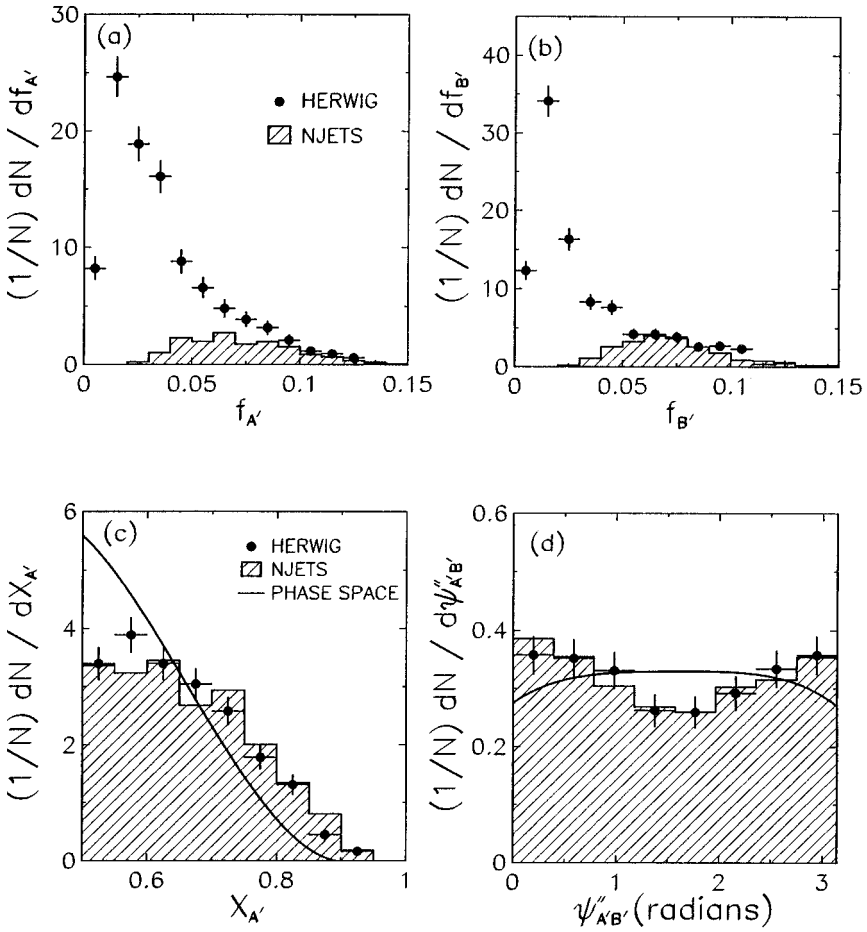

FIG. 17. The predicted distributions of the variables describing the $(A'B')$ system for five-jet events produced at the Fermilab proton-antiproton collider that satisfy the requirement $m_{5J}>750$ GeV/c^2. HERWIG predictions (points) are compared with NJETS predictions (histograms) and the phase-space model predictions (curves) for (a) $f_{A'}$, (b) $f_{B'}$, (c) $X_{A'}$, and (d) $\psi''_{A'B'}$.

more, for five-body configurations that approach a three-body topology, our five-jet parameters reduce to the three-jet variables discussed previously. Thus we will be able to compare the characteristics of five-jet events with the corresponding characteristics of three-jet and four-jet events.

The five-jet variables are shown schematically in Fig. 13. We begin by reducing the five-jet system to a four-body system by combining the two jets with the lowest two-jet mass. We will label the two jets we combine C and D, with $E_C>E_D$, where E_C and E_D are the jet energies in the five-jet restframe. We can then further reduce the resulting four-body system to a three-body system by combining the two bodies with the lowest two-body mass. We will label the two objects we combine A' and B', with $E_{A'}>E_{B'}$. After combining C with D, and then A' with B', the resulting three bodies are labeled $3''$, $4''$, and $5''$, and ordered so that $E_{3''}>E_{4''}>E_{5''}$. The double primes remind us that the objects are defined after two operations in which the two bodies with the lowest two-body mass have been combined. The three-body system can be completely specified using the variables: $X_{3''}$, $X_{4''}$, $\cos\theta_{3''}$, $\psi_{3''}$, $f_{3''}$, $f_{4''}$, and $f_{5''}$.

The NJETS and HERWIG predictions for the m_{5J} distribution are shown in Fig. 14 for five-jet events produced at the Fermilab proton-antiproton collider and satisfying the requirement $m_{5J}>750$ GeV/c^2. The QCD predictions for the $X_{3''}$, $X_{4''}$, $\cos\theta_{3''}$, and $\psi_{3''}$ distributions are compared with the phase-space model predictions in Fig. 15. The predicted distributions are qualitatively similar to the equivalent four-jet distributions shown in Fig. 10. Note that the QCD predictions for the $\cos\theta_{3''}$ distribution are remarkably similar to the simple LO $q\bar{q}\rightarrow q\bar{q}$ angular distribution. The HERWIG predictions for the normalized single-jet masses $f_{j''}$ are shown in Fig. 16. Once again, the HERWIG and NJETS distributions are in agreement at large mass fractions.

We must now specify the intermediate four-body system. In analogy with the four-jet analysis we will do this by specifying four additional dimensionless variables that describe the $(A'B')$ system. We choose (a) the normalized masses $f_{A'}$ and $f_{B'}$, (b) $X_{A'}$, defined in the five-jet restframe as the fraction of the energy of the $(A'B')$ system taken by the leading body

$$X_{A'}\equiv\frac{E_{A'}}{E_{A'}+E_{B'}}, \tag{15}$$

and (c) $\psi''_{A'B'}$, defined in the five-jet restframe as the angle between (i) the plane containing the $(A'B')$ system and the average beam direction, and (ii) the plane containing A' and B' (see Fig. 13). Note that

$$\cos\psi''_{A'B'}\equiv\frac{(\vec{P}_{A'}\times\vec{P}_{B'})\cdot(\vec{P}_{A'B'}\times\vec{P}_{\rm av})}{|\vec{P}_{A'}\times\vec{P}_{B'}||\vec{P}_{A'B'}\times\vec{P}_{\rm av}|}. \tag{16}$$

The predicted distributions of these variables are shown in Fig. 17. The HERWIG predictions for the $f_{A'}$ and $f_{B'}$ distributions peak at values of about 0.02 and have long tails associated with composite A' or B' systems. The tails are

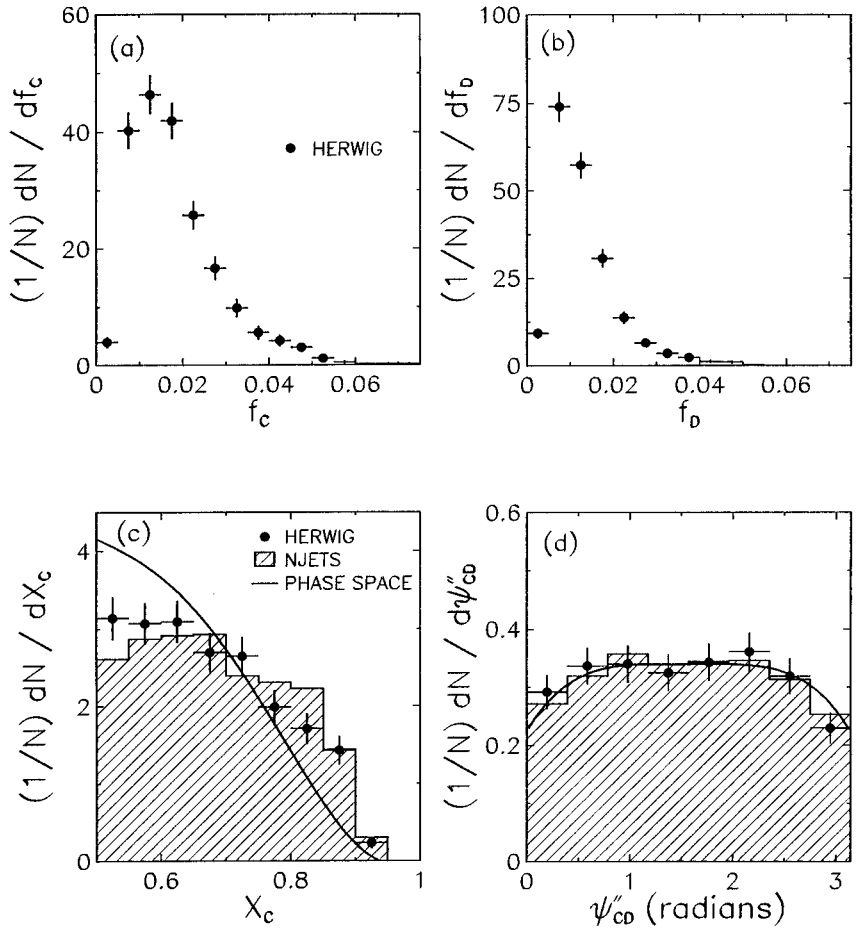

FIG. 18. The predicted distributions of the variables describing the (CD) system for five-jet events produced at the Fermilab proton-antiproton collider that satisfy the requirement $m_{5J}>750$ GeV/c^2. HERWIG predictions (points) are compared with NJETS predictions (histograms) and the phase-space model predictions (curves) for (a) f_C, (b) f_D, (c) X_C, and (d) ψ''_{CD}.

accounted for by the NJETS predictions. It is interesting to compare the $X_{A'}$ and $\psi''_{A'B'}$ distributions with the corresponding four-jet distributions [Figs. 12(c) and 12(d), respectively]. The QCD and phase-space model predictions for the five-jet distributions are qualitatively similar to the corresponding four-jet distributions. Note that the HERWIG and NJETS predictions are in general agreement with one another.

Finally, to complete our specification of the five-jet system we must define a further four variables that describe the two-body (CD) system. We choose the single-jet mass fractions f_C and f_D, and the variables X_C, and ψ''_{CD} defined by Eqs. (15) and (16) with the substitutions $A'\rightarrow C$ and $B'\rightarrow D$. The predicted distributions of these variables are shown in Fig. 18. The HERWIG predictions for the f_C and f_D distributions peak at values less than 0.02. Note that the QCD predictions for the X_C distribution are harder than the corresponding phase-space model prediction, whilst the QCD predictions for the ψ''_{CD} distribution are similar to the corresponding phase-space model prediction.

We conclude by noting that we have defined 16 variables that specify a five-jet system in the five-body restframe: m_{5J}, $X_{3''}$, $X_{4''}$, $\cos\theta_{3''}$, $\psi_{3''}$, $f_{3''}$, $f_{4''}$ $f_{5''}$, $f_{A'}$, $f_{B'}$, $X_{A'}$, $\psi''_{A'B'}$, f_C, f_D, X_C, and ψ''_{CD}.

VII. GENERALIZATION TO EVENTS WITH SIX OR MORE JETS

A list of the multijet variables described in the preceding sections is given in Table I. The extension of the variables to describe multijet systems with more than five jets is straightforward. As an example the variables required to describe a six-jet event are also listed in Table I. In general, to describe an event containing N jets we use the mass of the N-jet system plus $(4N-5)$ dimensionless variables. To define the dimensionless variables we proceed by reducing the N jet system to a three-body system. This is done in $(N-3)$ steps. In each step the two bodies with the lowest two-body mass are combined by adding the two four-vectors. The resulting three-body system is described by specifying seven parameters, namely the normalized masses of the three bodies (e.g., f_3, f_4, and f_5), the Dalitz variables for the two leading bodies (e.g., X_3 and X_4), the cosine of the leading-body scattering angle (e.g., $\cos\theta_3$), and the angle between the three-body plane and the beam direction (e.g., ψ_3). To complete the description of the N-jet system we must then specify an additional four parameters for each step in which two bodies were combined. These parameters are the normalized masses of the two bodies (e..g, f_A and f_B), the fraction of the two-body energy taken by the leading body (e.g., X_A), and the angle defined in the N-jet restframe between the plane containing the two-body system and the beam direction and the plane defined by the two bodies (e.g., ψ'_{AB}).

VIII. SUMMARY

A set of $(4N-4)$ parameters have been defined that can be used to analyze events in which N jets have been produced in high-energy hadron-hadron collisions. These multi-

TABLE I. Summary of the $(4N-4)$ multijet variables for $N=2$, 3, 4, 5, and 6.

Two jet	Three jet	Four jet	Five jet	Six jet
m_{2J}	m_{3J}	m_{4J}	m_{5J}	m_{6J}
$\cos\theta^*$	$\cos\theta_3$	$\cos\theta_{3'}$	$\cos\theta_{3''}$	$\cos\theta_{3'''}$
f_3	f_3	$f_{3'}$	$f_{3''}$	$f_{3'''}$
f_4	f_4	$f_{4'}$	$f_{4''}$	$f_{4'''}$
	f_5	$f_{5'}$	$f_{5''}$	$f_{5'''}$
	ψ_3	$\psi_{3'}$	$\psi_{3''}$	$\psi_{3'''}$
	X_3	$X_{3'}$	$X_{3''}$	$X_{3'''}$
	X_4	$X_{4'}$	$X_{4''}$	$X_{4'''}$
		f_A	$f_{A'}$	$f_{A''}$
		f_B	$f_{B'}$	$f_{B''}$
		X_A	$X_{A'}$	$X_{A''}$
		ψ'_{AB}	$\psi''_{A'B'}$	$\psi'''_{A''B''}$
			f_C	$f_{C'}$
			f_D	$f_{D'}$
			X_C	$X_{C'}$
			ψ''_{CD}	$\psi'''_{C'D'}$
				f_E
				f_F
				X_E
				ψ'''_{EF}

jet parameters span the multijet parameter space, and make it possible to compare the characteristics of events having N jets with the characteristics of events having for example $(N+1)$ jets. To illustrate the use of the multijet variables described in this paper, QCD and phase-space model predictions have been compared for three-jet, four-jet, and five-jet events produced at the Fermilab proton-antiproton collider. For this particular example we find the following.

(i) The parton shower Monte Carlo predictions for the shapes of the single-differential distributions that correspond to a complete set of multijet variables are generally in agreement with the corresponding QCD LO $2\rightarrow N$ matrix element predictions. This general agreement is seen for all of the distributions except for the single-body mass fraction distributions where the absence of a fragmentation model in the NJETS calculation makes the comparison inappropriate.

(ii) In more detail, there are some differences between the NJETS and HERWIG predictions. In particular, we find that a statistical comparison between the two sets of QCD predictions yields a χ^2 per degree of freedom greater than 2 for several of the distributions (X_3, X_4, ψ_3, $X_{4'}$, X_A, $\cos\theta_{3''}$, and $\psi_{3''}$). It is therefore possible that a comparison of measured multijet distributions with predictions from LO QCD $2\rightarrow N$ matrix element calculations and from parton shower Monte Carlo calculations, may show a preference for one of the two calculations.

(iii) There are striking similarities between many of the $(N+1)$-jet distributions with the equivalent N-jet distributions. Several sets of distributions have shapes that are almost independent of N once the differences in the phase-space distributions have been taken into account. The multijet mass distributions $(m_{2J},m_{3J},m_{4J},m_{5J})$, leading-body angular distributions $(\cos\theta^*,\cos\theta_3,\cos\theta_{3'},\cos\theta_{3''})$, and the two-body energy sharing distributions $(X_A,X_{A'},X_C)$ have very little dependence on N after taking into account the differences in the phase-space distributions. The other three-body angular distributions $(\psi_3,\psi_{3'},\psi_{3''})$, leading-body Dalitz variable distributions $(X_3,X_{3'},X_{3''})$, next-to-leading-body Dalitz variable distributions $(X_4,X_{4'},X_{4''})$, and two-body angular distributions $(\psi'_{AB},\psi''_{CD},\psi''_{A'B'})$ vary only slowly with N. These similarities could be exploited to provide a check of present and future multijet calculations for large N where complete LO matrix element calculations are not available and approximations must therefore be used.

ACKNOWLEDGMENTS

We are grateful to Walter Giele for many interesting discussions. This work was supported by the U.S. Department of Energy, and the Ministry of Science, Culture and Education of Japan.

[1] CDF Collaboration, F. Abe *et al.*, Phys. Rev. Lett. **75**, 608 (1995).

[2] F. A. Berends *et al.*, Phys. Lett. **118B**, 124 (1981); Z. Kunst and E. Pietarinen, Nucl. Phys. **B164**, 45 (1980); T. Gottschalk and D. Sivers, Phys. Rev. D **21**, 102 (1980).

[3] J. Gunion and Z. Kunst, Phys. Lett. **159B**, 167 (1985); S. Parke and T. Taylor, Nucl. Phys. **B269**, 410 (1986); Z. Kunst, *ibid.* **B271**, 333 (1986); J. Gunion and Z. Kunst, Phys. Lett. B **176**, 163 (1986); J. Gunion and J. Kalinowski, Phys. Rev. D **34**, 2119 (1986); S. Parke and T. Taylor, *ibid.* **35**, 313 (1987); F. A. Berends and W. T. Giele, Nucl. Phys. **B294**, 700 (1987); M. Mangano, S. Parke, and Z. Xu, *ibid.* **B298**, 673 (1988); M. Mangano and S. Parke, *ibid.* **B299**, 190 (1987).

[4] F. A. Berends, W. T. Giele, and H. Kuijf, Nucl. Phys. **B333**, 120 (1990); F. A. Berends and H. Kuijf, *ibid.* **B353**, 59 (1991).

[5] F. A. Berends, W. T. Giele, and H. Kuijf, Phys. Lett. B **232**, 266 (1989).

[6] F. A. Berends and W. T. Giele, Nucl. Phys. **B306**, 759 (1988).

[7] Z. Kunst and W. J. Stirling, Phys. Lett. B **171**, 307 (1986); Phys. Rev. D **56**, 2493 (1988); C. J. Maxwell, Phys. Lett. B **192**, 190 (1987); Nucl. Phys. **B316**, 321 (1989); S. J. Parke and T. R. Taylor, Phys. Rev. Lett. **56**, 2459 (1986); M. L. Mangano and S. J. Parke, Phys. Rev. D **39**, 758 (1989); C. J. Maxwell and S. J. Parke, *ibid.* **44**, 2727 (1991).

[8] UA1 Collaboration, G. Arnison *et al.*, Phys. Lett. **123B**, 115 (1983); **132B**, 214 (1983); **136B**, 294 (1984); Phys. Lett. B **177**, 244 (1986); UA1 Collaboration, C. Albajar *et al.*, *ibid.* **209**, 127 (1988).

[9] UA1 Collaboration, G. Arnison *et al.*, Phys. Lett. **158B**, 494 (1985).

[10] UA2 Collaboration, M. Banner *et al.*, Phys. Lett. **118B**, 203 (1982); UA2 Collaboration, P. Bagnaia *et al.*, *ibid.* **138B**, 430 (1984); **144B**, 283 (1984); UA2 Collaboration, J. A. Appel *et al.*, *ibid.* **165B**, 441 (1985); UA2 Collaboration, J. Alitti

et al., Z. Phys. C **49**, 17 (1991).
[11] UA2 Collaboration, J. A. Appel *et al.*, Z. Phys. C **30**, 341 (1986).
[12] CDF Collaboration, F. Abe *et al.*, Phys. Rev. Lett. **62**, 3020 (1989); **64**, 157 (1990); **69**, 2896 (1992); **71**, 2542 (1993); Phys. Rev. D **41**, 1722 (1990); **48**, 998 (1993).
[13] CDF Collaboration, F. Abe *et al.*, Phys. Rev. D **45**, 1448 (1992).
[14] D0 Collaboration, S. Abachi *et al.*, Fermilab Report No. FERMILAB Conf-95/214-E, 1995 (unpublished).
[15] UA2 Collaboration, J. Alitti *et al.*, Phys. Lett. B **268**, 145 (1991).
[16] CDF Collaboration, F. Abe *et al.*, Phys. Rev. D **47**, 4857 (1993).
[17] G. Marchesini and B. Webber, Nucl. Phys. **B310**, 461 (1988).
[18] H. L. Lai *et al.*, Phys. Rev. D **51**, 4763 (1995).
[19] A. D. Martin, R. G. Roberts, and W. J. Stirling, Phys. Lett. B **306**, 145 (1993).
[20] J. Collins and D. Soper, Phys. Rev. D **16**, 2219 (1977).
[21] B. L. Combridge and C. J. Maxwell, Nucl. Phys. **B239**, 429 (1984).